Effect of Mo Doping on the Room-Temperature Structure of Vanadium Sesquioxide

C. Tenailleau,[†] E. Suard,[‡] J. Rodriguez-Carvajal,[§] M.-P. Crosnier-Lopez,[†] and P. Lacorre*,[†]

Laboratoire des Fluorures, UMR CNRS 6010, Université du Maine, F-72085 Le Mans Cedex 9, France, Institut Laue Langevin, Avenue des Martyrs, B.P. 156, F-38042 Grenoble Cedex 9, France, and Laboratoire Léon Brillouin (CEA-CNRS), Centre d'Etudes de Saclay, F-91191 Gif-sur-Yvette Cedex, France

Received February 1, 2002. Revised Manuscript Received May 31, 2002

The room-temperature crystal structure of $(V_{1-x}Mo_x)_2O_3$ ($0 \le x \le 0.20$) is studied in detail, using combined X-ray and neutron powder diffraction. Substitution of vanadium by molybdenum tends to regularize the atomic stacking and reduce octahedral distortion. Cation−anion distances increase with x, in a way that is consistent with a trivalent oxidation state of both molybdenum and vanadium. Quite unexpectedly, such an octahedral and volume expansion is accompanied by a regular decrease of nearest- and next-nearest-neighbor cation−cation distances. This behavior is discussed in terms of a possible progressive establishment of metal−metal bonding and with respect to the stabilization of the metallic phase.

Introduction

Vanadium sesquioxide, which exhibits a wide resistivity gap metal/insulator transition[1,2] around 160 K, has always been considered as a typical example of oxide sustaining a Mott transition.[3] A tremendous amount of work has been devoted to V_2O_3 that appears to be a borderline material and to its doped counterparts (see, for instance, refs 4 and 5 and references therein). The effect of cationic substitution is to stabilize either the insulating phase (as with Cr^{3+}, with a kind of reentrant metallic behavior) or the metallic one (as with Ti^{3+}).[6] Despite the very numerous studies carried out for half of a century on this fascinating family of oxides and their structural and physical properties, no global understanding of the system has emerged yet.

Structurally speaking, the room-temperature metallic phase of V_2O_3 is isostructural to corundum with rhombohedral symmetry (space group $R\bar{3}c$), while the low-temperature insulating phase presents a monoclinic distortion. The corundum structure can be described as a pseudocompact ABAB stacking of oxygen layers along the c hexagonal axis, defining octahedral layers $^2/_3$ occupied by cations (see Figure 1). An ideal close-compact stacking would have an hexagonal c/a ratio equal to $2\sqrt{2}$, which happens to be the case of V_2O_3 with a ratio $c/a = 2.828$ at room temperature.[7] However, V_2O_3 represents a singularity in the metal oxide series with a corundum-type structure because it has the largest c/a ratio;[6] as a consequence the effect of any known doping up to now was to reduce the c/a ratio (applying pressure was the only known way[8] to increase the c/a ratio of V_2O_3). Recently, we have presented a new possibility of doping for vanadium sesquioxide, with an element of the second-transition-metal series, molybdenum.[9] As shown in the previous paper, it appears that the effect of molybdenum doping on the V_2O_3 cell parameters is opposite to that of any other known doping, with increasing c parameter while a decreases, thus leading to an increase of the c/a ratio and cell volume. Conversely, the metal/insulator transition temperature is reduced by Mo doping, and above a certain level (around 6% doping), the transition is suppressed. This result[9] allowed us to invalidate a previous assumption that above a certain critical value of the c parameter the insulating phase would be stabilized.[10] Such unexpected behavior prompted us to examine more closely the effect of Mo doping on the crystal structure of vanadium sesquioxide and to compare it with those of already known doping such as with Ti or Cr. The results of this study are presented below.

Experimental Section

Synthesis. The synthesis process has been described elsewhere in detail.[9] Small amounts of stoichiometric powder mixtures of V_2O_3 and MoO_2 were heated in a high-frequency induction furnace under vacuum (about 10^{-6} mbar) at 870 °C.

* To whom correspondence should be addressed. E-mail: philippe.lacorre@univ-lemans.fr.
[†] Université du Maine.
[‡] Institut Laue Langevin.
[§] Centre d'Etudes de Saclay.

(1) Foex, M. *C. R. Acad. Sci.* **1946**, *223*, 1126.
(2) Foex, M. *C. R. Acad. Sci.* **1949**, *229*, 880.
(3) Mott, N. F. *Proc. Phys. Soc. A* **1949**, *62*, 416.
(4) Honig, J. M. *J. Solid State Chem.* **1982**, *45*, 1.
(5) Yethiraj, M.*J. Solid State Chem.* **1990**, *88*, 53.
(6) McWhan, D. B.; Rice, T. M.; Remeika, J. P. *Phys. Rev. Lett.* **1969**, *23*, 1384.
(7) McWhan, D. B.; Remeika, J. P. *Phys. Rev. B* **1970**, *2*, 3734.
(8) Finger, L. W.; Hazen, R. M. *J. Appl. Phys.* **1980**, *51*, 5362.
(9) Lacorre, P.; Tenailleau, C. *Solid State Sci.* **2002**, *4*, 217.
(10) Ueda, Y.; Kosuge, K.; Kachi, S. *J. Solid State Chem.* **1980**, *31*, 171.

10.1021/cm021127l CCC: $22.00
Published on Web 07/16/2002

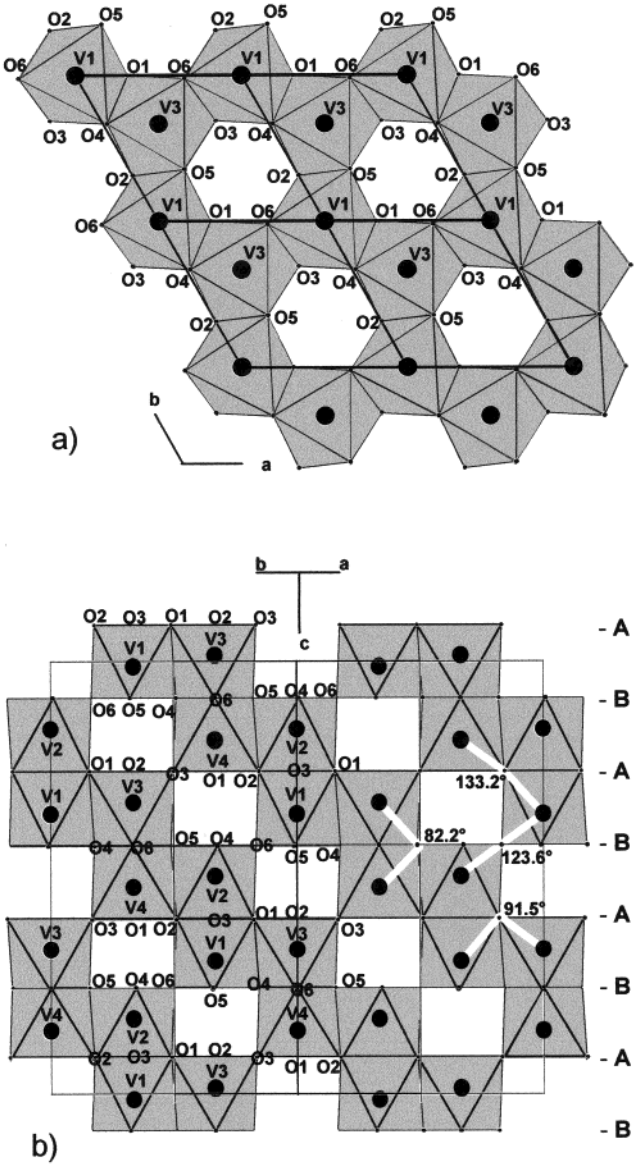

Figure 1. Crystal structure of V_2O_3: view of a hexagonal plane (a) and perpendicularly to it (b).

This process was repeated several times after intermediate grindings for several samples in order to get large amounts (several grams) of pure materials. Reaction takes progressively place through the formation of an intermediate phase $Mo_{1-y}V_yO_2$. For larger Mo content (typically $x = 0.2$), $Mo_{1-y}V_yO_2$, prepared from a stoichiometric mixture of V_2O_5, MoO_3, and Mo heated in a sealed evacuated silica tube at 640 and 1000 °C, was used as the starting material. The appropriate mixture of V_2O_3 and $Mo_{1-y}V_yO_2$ was then placed in the induction furnace and heated as above. The advancement of the reactions and the purity of the phases were checked by X-ray diffraction. The prepared samples were kept in a glovebox with a controlled atmosphere (less than 10 ppm of oxygen).

Structural Characterization. The structural characterization was carried out using both powder X-ray and neutron diffraction. X-ray diffraction patterns were recorded on a Bragg−Brentano diffractometer (Bruker D8 AXS, Cu Kα, 2θ domain 20−140°, step 0.02°, time/step 15 s) and the neutron diffraction patterns on Debye−Scherrer diffractometers D2B (ILL Grenoble, $\lambda = 1.5941$ Å, 2θ domain 10−158°, step 0.05°, five scans 85 000 or 95 000 counts) for $x = 0$, 3, 5, and 10% and 3T2 (LLB Saclay, $\lambda = 1.2252$ Å, 2θ domain 10−125.45°, step 0.05°, scan 50 000 or 80 000 counts) for $x = 2$, 4, and 20%. Molybdenum is easily detectable by both techniques but is present in small amounts in most samples. Concerning the other ions, X-rays are more sensitive to vanadium (scattering sections $f_x = 5.63$ and $2.82\ 10^{-12}$ cm for V^{3+} and O^{2-}, respectively) and neutrons much more sensitive to oxygen, with vanadium being practically undetectable (Fermi lengths $b = -0.051$ and $+0.577 \times 10^{-12}$ cm for V and O, respectively).[11] For this reason we used coupled refinement of X-rays and neutron diffraction patterns recorded at room temperature. The Rietveld program FullProf[12] was used for structural refinement. Preliminary tests showed that a 50:50% weighting scheme for X-rays−neutrons contribution was the best compromise for optimal reliability factors. Figure 2 gives a typical example of refined patterns ($x = 3\%$).

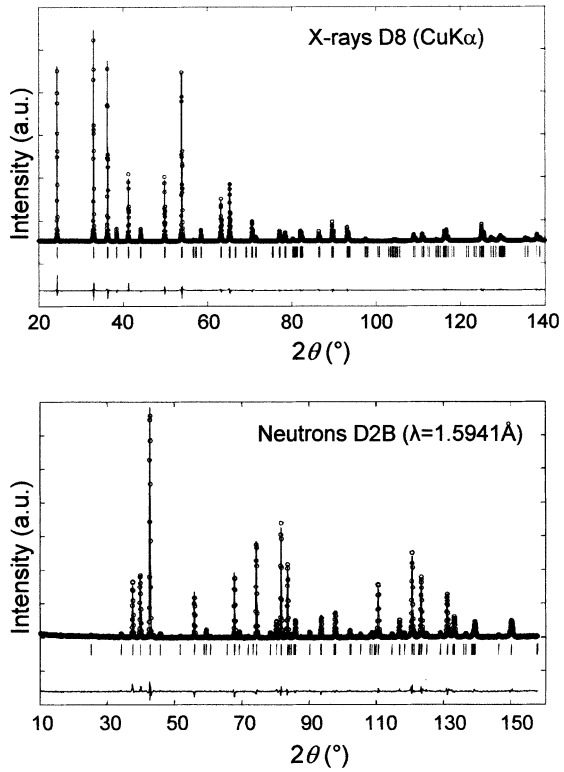

Figure 2. X-ray (above) and neutron (below) diffraction patterns of $(V_{0.97}Mo_{0.03})_2O_3$ (observed = dots, calculated = lines, difference below) after coupled 50:50% X-ray/neutron Rietveld refinements. Reliability factors for X-rays: $R_p = 0.104$, $R_{wp} = 0.135$, $R_{exp} = 0.085$, $\chi^2 = 2.53$, $R_B = 0.037$, and $R_F = 0.039$. Reliability factors for neutrons: $R_p = 0.123$, $R_{wp} = 0.112$, $R_{exp} = 0.066$, $\chi^2 = 2.90$, $R_B = 0.047$, and $R_F = 0.037$.

Results and Discussion

Crystal Structure. The structural refinements were carried out using the space group $R\bar{3}c$ and starting from the known atomic positions of pure V_2O_3. In the hexagonal setting, cations (C) are located on a 12c site with coordinates (0, 0, z) and z close to 0.346, while oxygen atoms (O) are on a 18e site with coordinates (x, 0, $^1/_4$) and x close to 0.312 (note that for a perfect close-compact stacking, $x(O) = z(C) = {}^1/_3$, with $c/a = 2\sqrt{2}$). For the pure V_2O_3 powder compound (see Table 1), cell parameters and atomic positions are very close to those published in the literature from single-crystal data.[13] For Mo-doped compounds, molybdenum was located at the same position as vanadium, and we checked for any

(11) Bacon, G. E. *Neutron diffraction*, 2nd ed.; Clarendon Press: Oxford, 1967.
(12) Rodriguez-Carvajal, J. *Physica (Amsterdam)* **1993**, *192B*, 55.
(13) Robinson, W. R. *Acta Crystallogr.* **1975**, *B31*, 1153.

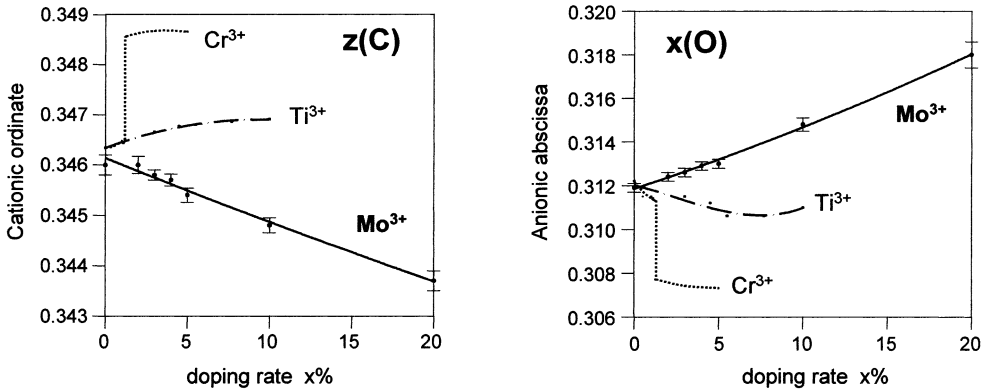

Figure 3. Atomic position parameters evolution upon doping of V_2O_3: comparison of Mo doping (full line, this work) with Ti and Cr doping (dashed and dotted lines, respectively, from ref 20).

Table 1. Results of the X-ray and Neutron Powder Diffraction Refinements of $(V_{1-x}Mo_x)_{2-\delta}O_3$

x	a (Å)	c (Å)	z(C)	B(C) (Å^2)	x(O)	B(O) (Å^2)
0	4.9525(4)	14.0038(2)	0.3460(1)	0.18(3)	0.3119(2)	0.43(2)
0.02	4.9508(4)	14.0316(2)	0.3460(1)	0.69(2)	0.3124(2)	0.35(2)
0.03	4.9499(4)	14.0431(2)	0.3458(1)	0.66(3)	0.3126(2)	0.55(2)
0.04	4.9478(5)	14.0697(2)	0.3457(1)	0.68(3)	0.3129(2)	0.40(2)
0.05	4.9463(4)	14.0864(2)	0.3454(1)	0.90(3)	0.3130(2)	0.54(2)
0.10	4.9405(5)	14.1631(2)	0.3448(1)	0.65(3)	0.3148(3)	0.62(2)
0.20	4.9309(4)	14.2819(2)	0.3437(2)	0.67(5)	0.3180(6)	0.52(4)

unusual trends in the thermal factors that would be a sign of a different positioning in the coordination octahedron. Isotropic thermal factors appear to be larger for all doped compounds (see Table 1). This is a consequence of the chemical disorder between molybdenum and vanadium ions that gives rise to local distortions appearing in the average structure as a static contribution to the thermal parameters (displacement parameters). Using anisotropic factors during refinement, while slightly improving reliability factors, does not give any coherent trend in the distortion of thermal ellipsoids upon doping. Moreover, it does not modify the final atomic positioning, and it is the reason we only give results obtained with isotropic thermal factors. Table 1 displays the results of the structural refinements for all of the studied samples, while the evolution upon doping of the refinable atomic coordinates (z for cations and x for oxygen) is plotted in Figure 3. As can be clearly seen on this figure and consistently with the c/a behavior,[9] molybdenum produces the opposite effect on atomic displacements than that of both trivalent titanium and chromium and an effect similar to pressure. This is a rather unexpected result because pressure usually reduces bond lengths, whereas molybdenum, which is larger than vanadium, should normally expand bond lengths, as suggested by volume expansion. We will therefore examine more closely in the following the structural deformations induced by molybdenum.

Despite its apparent extreme simplicity relative to the small number of independent atomic positions (two) and refinable coordinates (one each) as seen above, the very symmetric arrangement of the corundum-type structure defines complex interatomic conformations. It is characterized by several kinds of subtly correlated interatomic distances and angles which control the transport and magnetic properties through orbital overlap. Cations are located on the threefold axes, off-centered in their coordination octahedra, with three short and three long distances to ligands due to electrostatic intercationic repulsion through the common face of bioctahedral units (see Figure 1). They define, along the hexagonal c axis, cationic pairs with the shortest cation−cation distances. Next-nearest cation neighbors lie in the hexagonal (a,b) plane in edge-sharing octahedra. As shown in Figure 1, there are four types of cation−anion−cation (superexchange) angles, slightly above 80° (face-sharing octahedra), 90° (edge-sharing octahedra), and 120−130° (corner-sharing octahedra). Figure 4 shows the evolution with the Mo doping rate of the main interatomic distances and angles (see also Table 2), together with those of Ti and Cr doping from the literature.

Oxidation State of Molybdenum. As mentioned in the Introduction, vanadium sesquioxide can sustain several types of substitution, either by isovalent (Al^{3+}, Sc^{3+}, Ti^{3+}, Cr^{3+}, and Fe^{3+}) or by aliovalent (Mg^{2+}, Ti^{4+}, V^{4+}, and Zr^{4+}) cations. V_2O_3 itself can easily be oxidized while keeping a cation-deficient $V_{2-\delta}O_3$ corundum-type structure whose metallic phase is stabilized when δ increases. The knowledge of the cationic oxidation state is therefore an important issue in order to have a better understanding of the properties of these materials. Using electron paramagnetic resonance spectroscopy, we have been able to detect the presence of V^{4+} ions in our samples and to quantify their proportion in samples kept in the glovebox and exposed to air.[14] In the samples used for this study, the maximal amount of V^{4+} ions measured after the diffraction experiments was lower than 0.03% relative to the total cationic amount, which is negligible compared to the doping level. Here we will focus on the molybdenum oxidation state through its incidence on the cationic radii as revealed by the evolution of average cation−oxygen distances upon doping.

Table 2 shows that these distances increase upon doping, a sign that the substituting cation is larger than trivalent vanadium. According to Shannon and Prewitt,[15] the ionic radius of trivalent vanadium is 0.64 Å, while those of trivalent and tetravalent molybdenum

(14) Tenailleau, C.; Kassiba, A.; Lacorre, P., to be published.
(15) Shannon, R. D.; Prewitt, C. T. *Acta Crystallogr.* **1969**, *B25*, 925.

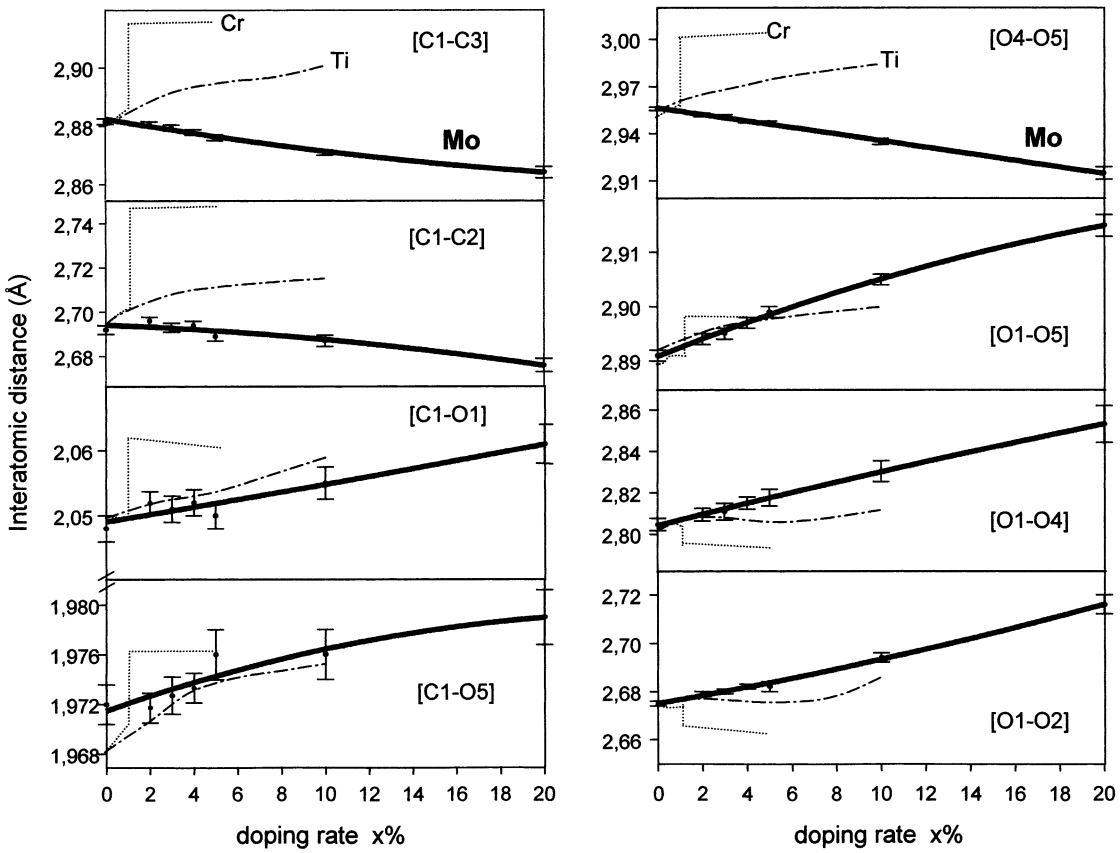

Figure 4. Evolution upon Mo doping of interatomic distances in $(V_{1-x}Mo_x)_2O_3$ (full line) and comparison with Ti and Cr doping (dashed and dotted lines, respectively, from ref 20).

Table 2. Room-Temperature Interatomic Distances and Angles in $(V_{1-x}Mo_x)_{2-\delta}O_3$ as a Function of *x*, from X-ray and Neutron Powder Diffraction Refinements[a]

distances (Å) and angles (deg)	$x = 0$	$x = 0.02$	$x = 0.03$	$x = 0.04$	$x = 0.05$	$x = 0.10$	$x = 0.20$
[C1−C2]	2.692(2)	2.696(1)	2.693(1)	2.694(1)	2.689(2)	2.687(2)	2.676(4)
[C1−C3]	2.8817(2)	2.8806(2)	2.8795(2)	2.8779(2)	2.8761(2)	2.8710(2)	2.8624(2)
[C1−O1]	2.048(1)	2.052(1)	2.051(1)	2.052(1)	2.050(1)	2.055(2)	2.061(3)
[C1−O5]	1.972(1)	1.972(1)	1.973(1)	1.973(1)	1.976(1)	1.976(1)	1.979(2)
[O1−O2]	2.675(1)	2.679(1)	2.680(1)	2.682(1)	2.682(1)	2.694(2)	2.716(4)
[O1−O4]	2.8049(3)	2.8095(3)	2.8110(4)	2.8151(3)	2.8176(4)	2.8308(5)	2.8531(9)
[O1−O5]	2.891(1)	2.894(1)	2.895(1)	2.897(1)	2.899(1)	2.905(1)	2.915(2)
[O4−O5]	2.956(1)	2.952(1)	2.951(1)	2.948(1)	2.947(1)	2.935(2)	2.914(4)
⟨O1−C1−O2⟩	81.56(7)	81.54(6)	81.59(7)	81.62(6)	81.71(7)	81.91(9)	82.41(16)
⟨O1−C1−O4⟩	88.46(4)	88.57(4)	88.63(5)	88.74(4)	88.83(5)	89.19(6)	89.81(10)
⟨O1−C1−O5⟩	91.95(4)	91.98(4)	92.01(5)	92.05(4)	92.13(5)	92.20(6)	92.13(10)
⟨O1−C1−O6⟩	168.77(9)	168.85(8)	168.98(9)	169.13(8)	169.35(9)	169.93(12)	171.10(22)
⟨O4−C1−O5⟩	97.05(3)	96.94(3)	96.82(7)	96.66(6)	96.45(7)	95.90(10)	94.84(18)
⟨C1−O1−C2⟩	82.09(9)	82.12(8)	82.04(9)	82.00(9)	81.89(9)	81.62(11)	80.95(18)
⟨C1−O1−C3⟩	91.54(4)	91.43(4)	91.37(5)	91.26(4)	91.17(5)	90.81(6)	90.18(10)
⟨C1−O6−C2⟩	123.62(7)	123.80(6)	123.89(7)	124.05(7)	124.17(8)	124.84(9)	126.07(14)
⟨C2−O1−C3⟩	133.28(8)	133.27(7)	133.29(8)	133.31(8)	133.38(9)	133.37(9)	133.36(16)

[a] Numbering of cations (C) and oxygen (O) corresponds to those adopted in Figures 1, 7, and 10.

are 0.69 and 0.65 Å, respectively. In our compounds, average cation−anion distances should follow

$$d_{C-O} = (1 - x)d_{V-O} + xd_{Mo-O}$$

that is

$$d_{C-O} = d_{V-O} + x[R(Mo) - R(V)]$$

where R(Mo) and R(V) represent the Mo and V radii, respectively.

A linear fit of the evolution of C−O cation−anion distances with the doping rate gives

$$d_{C-O} = 2.01056 + 0.04789x \text{ Å}$$

with a very good reliability ($r^2 = 0.991$; see Figure 5). Hence, R(Mo) = R(V) + 0.048 Å = 0.688 Å.

The molybdenum radius in our compounds is thus very close to that of trivalent molybdenum, and as can be seen on Figure 5 through the very small dispersion of data points, the accuracy of this measurement is much higher than would be expected from the distance

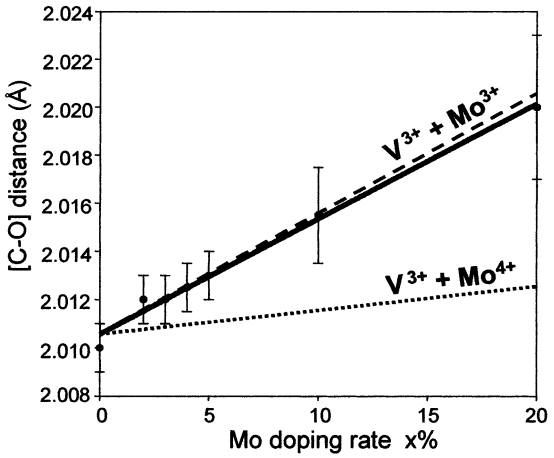

Figure 5. Influence of Mo doping on the average nearest-neighbor cation−anion distances in vanadium sesquioxide (dots and fitted full line). Comparison with the theoretical evolution assuming trivalent (dashed) and tetravalent (dotted) molybdenum.

standard deviations. The presence of divalent vanadium or molybdenum, which cannot be excluded on crystallographic grounds only, is very unlikely for several reasons:

(a) Both cations are much larger than trivalent vanadium [$R(V^{2+}) = 0.79$ Å], and therefore their incorporation in the corundum-type lattice is probably very difficult; as a matter of fact, no mention has been given in the literature of the existence of a reduced form of V_2O_3.

(b) It would mean the simultaneous presence, at the intermediate stage of the synthesis process where the $Mo_{1-y}V_yO_2$ phase is present, of V^{2+} and V^{4+} or Mo^{2+} and Mo^{4+} in the samples.

Therefore and to a good accuracy, one can deduce that, in our $(V_{1-x}Mo_x)_{2-\delta}O_3$ samples, δ is very close to zero, with both vanadium and molybdenum being mostly in the trivalent state.

Structural Modification upon Doping. A deeper analysis of the octahedral distortion upon doping shows that molybdenum makes atomic stacking and oxygen octahedra more regular. It can be seen from the cationic−anionic coordinates getting closer to $^1/_3$ (see Table 1 or Figure 3). The sizes of full and empty octahedra tend to equalize, as can be seen in Figure 6 from opposite [O−O] distances. In addition, the sizes of the octahedral faces perpendicular to the *c* hexagonal axis tend also to equalize: smaller common faces of bioctahedral units enlarge, while opposite larger faces shrink (see Figure 7). With the general expansion of full octahedra upon Mo doping, cations move closer to the octahedral barycenter (Figure 8). The distortion of occupied octahedra can be estimated from the deviation of interatomic distances and angles relative to a perfect octahedron, as measured for instance by $(\Sigma|d - d_0|)/\Sigma d_0$, where d is an interatomic distance [O−O] or angle ⟨O−C−O⟩ and d_0 the average distance, or 90° or 180° for angles. The evolution with Mo doping of such deviations is plotted on Figure 9, which clearly shows an overall decrease of distortion when x increases in $(V_{1-x}Mo_x)_2O_3$.

Another important structural effect of Mo doping is that, despite general expansion of cation−anion distances, all nearest-neighbor cation−cation distances decrease (see Figure 4). This behavior, somewhat unexpected in consideration of Mo^{3+} and V^{3+} cationic sizes (see above), will be discussed in the next section.

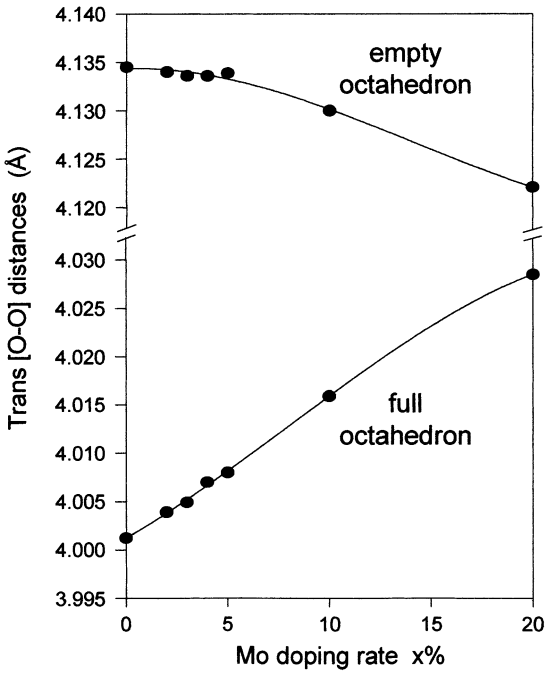

Figure 6. Evolution of the octahedral sizes with Mo doping in $(V_{1-x}Mo_x)_2O_3$.

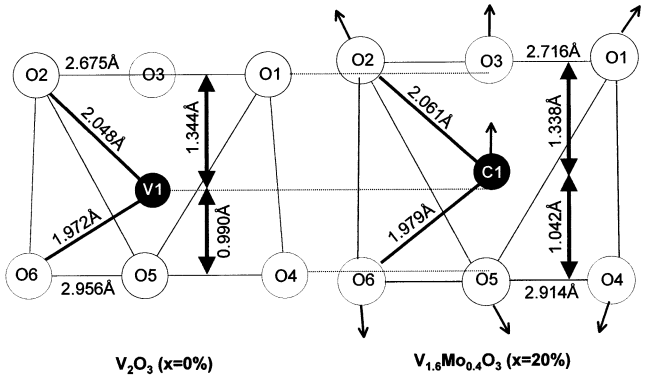

Figure 7. Effect of Mo doping on the relative atomic positioning in a full octahedron of $(V_{1-x}Mo_x)_2O_3$ (slightly exaggerated in the right octahedron).

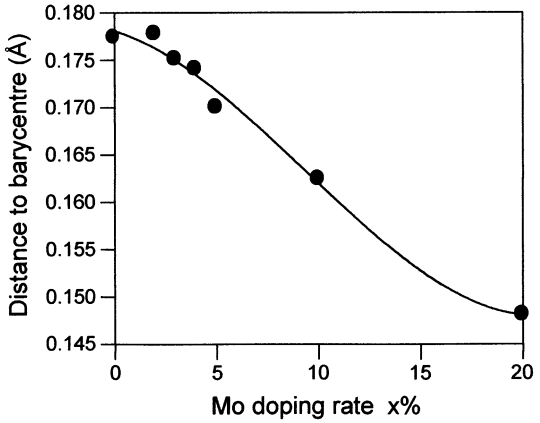

Figure 8. Distance from a cation to its octahedron barycenter in $(V_{1-x}Mo_x)_2O_3$ as a function of x.

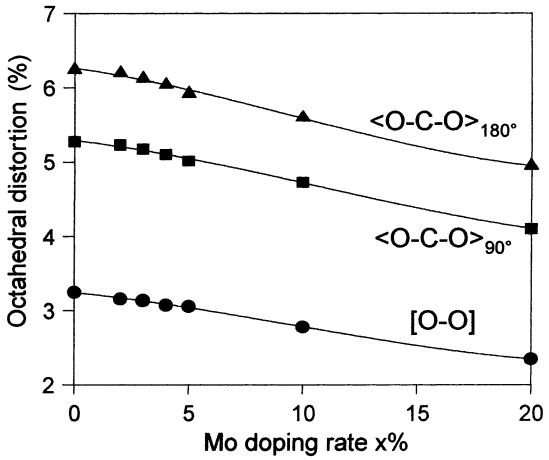

Figure 9. Decrease of octahedral distortion with x in $(V_{1-x}Mo_x)_2O_3$ (see text for definitions).

Figure 10 gives an overview of the different atomic movements upon substitution, in the hexagonal (a,b) plane and perpendicularly to it. It can be seen that cations get closer to the empty octahedral site in the hexagonal plane and closer to each other within bioctahedral units perpendicular to the hexagonal plane.

Discussion. The oxidation states of vanadium and molybdenum in $(V_{1-x}Mo_x)_{2-\delta}O_3$ are very close to +3, which gives us some hints on the way the complex synthesis process takes place in the high-vacuum furnace with V_2O_3 and MoO_2 as starting materials. As described earlier,[9] an intermediate reaction phase has been detected as being $Mo_{1-y}V_yO_2$, aside from partly reacted $(V_{1-x}Mo_x)_{2-\delta}O_3$. This means that a first reaction step occurs through a fast oxidoreduction process ($yMo^{4+} + yV^{3+} \rightarrow yMo^{3+} + yV^{4+}$) involving part of MoO_2, which oxidizes a small part of V_2O_3 to VO_2 that reacts with remaining MoO_2 to form $Mo_{1-y}V_yO_2$. The remaining V_2O_3 reacts with Mo^{3+} to form partly substituted $(V_{1-x}Mo_x)_{2-\delta}O_3$. The second reaction step involves the progressive reduction under vacuum of $Mo_{1-y}V_yO_2$ with its incorporation in $(V_{1-x}Mo_x)_{2-\delta}O_3$. The complexity of such a process explains the difficulty of samples preparation. Moreover, oxidation of trivalent vanadium at the contact (and the expense) of tetravalent molybdenum shows that, in these phases, vanadium oxidizes probably more easily than molybdenum.

An intriguing point of the crystal structure evolution upon doping is the progressive decrease of the nearest-neighbor cation−cation distances, despite the larger size of trivalent molybdenum relative to that of trivalent vanadium. The origin of it might be the progressive establishment of molybdenum metal−metal bonding. Such a type of bonding is mainly observed in early transition metals with d^1 electronic configuration but also with d^2 or d^3 configuration for 4d and 5d series (ref 16, p 19). A typical example is provided by titanium sesquioxide that is isostructural to V_2O_3. Trivalent titanium is a $3d^1$ cation. In the high-temperature metallic form of Ti_2O_3, a decrease of nearest-neighbor Ti−Ti distances is observed when the temperature is cooled to room temperature. When a critical Ti−Ti distance is reached, on the order of interatomic distances in the metal, Ti_2O_3 becomes insulating because of the opening of a gap between bonding (a_{1g} orbitals along the c hexagonal axis in the bioctahedral units) and antibonding ($e_g\pi$ orbitals in the hexagonal planes) levels, accompanying metal−metal bonding. Trivalent molybdenum is a $4d^3$ cation, therefore possibly susceptible to metal−metal bonding as already evidenced in oxides[17,18] and chlorides.[19] The decrease of cation−cation distances observed in $(V_{1-x}Mo_x)_2O_3$ might thus be due to the progressive setting of metal−metal bonding within Mo clusters, whose probability increases with the doping rate. In $(V_{1-x}Mo_x)_2O_3$, however, the critical distance is not reached because the metallic phase persists.

The stabilization of the metallic phase might appear to be contradictory with the metal−metal bonding hypothesis, but it could be qualitatively explained in the same way as has been done for Ti^{3+} and Cr^{3+} doping, through the influence of relative orbital overlaps (ref 16, p 227). Titanium 3d orbitals are more extended than vanadium orbitals, and this stronger overlap increases the overall bandwidth, thus stabilizing the metallic state. Chromium has an opposite effect because of more contracted orbitals, with weaker overlap and narrower bandwidth destabilizing the metallic state. In our case, molybdenum 4d orbitals have a larger spatial extension than vanadium 3d orbitals and tend to increase overlap and bandwidth and to stabilize the metallic phase. The decrease of nearest-neighbor cation−cation distances upon doping in $(V_{1-x}Mo_x)_2O_3$ is an additional favorable factor.

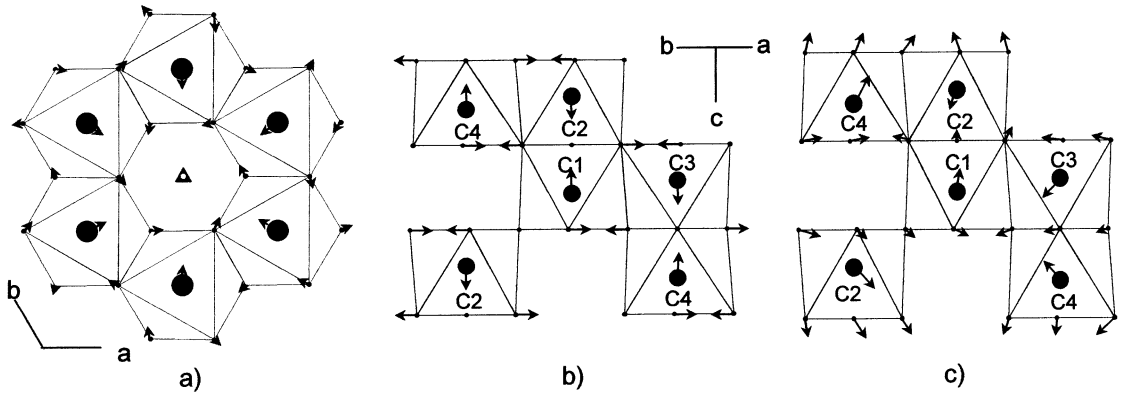

Figure 10. General atomic shifts upon Mo doping in vanadium sesquioxide in the hexagonal plane (a) and perpendicularly to it (b, from reduced coordinates only, and c, real atomic displacements taking account of the cell expansion).

Conclusion

The detailed evolution of the room-temperature crystal structure of V_2O_3 upon doping by Mo^{3+} has been presented and discussed. The structural effect of Mo doping is different from any other effect: on the one hand, similar to Cr and Ti effects for cation−anion distances and cell volume and, on the other hand, similar to the pressure effect for the *c*/*a* ratio and cation−cation distances. Yet, Mo doping stabilizes the metallic phase, as do Ti doping and pressure. It is expected that the present study will help in the understanding of the intriguing properties of the vanadium sesquioxide sys-tem. It will be completed soon by a similar study carried out at low temperature, above the metal−insulator transition and below it in the insulating monoclinic phase. The physical properties of this new family of vanadium sesquioxides will also be studied.

CM021127L

(16) Cox, P. A. *Transition metal oxides: an introduction to their electronic structure and properties*; Clarendon Press: Oxford, 1995.

(17) Wang, S. L.; Wang, C. C.; Lii, K. H. *J. Solid State Chem.* **1988**, *74*, 409.

(18) Lii, K. H.; Wang, C. C.; Wang, S. L. *J. Solid State Chem.* **1988**, *77*, 407.

(19) Stranger, R.; Grey, I. E.; Madsen, I. C.; Smith, P. W. *J. Solid State Chem.* **1987**, *69*, 162.

(20) Chen, C.; Hahn, J. E.; Rice, C. E.; Robinson, W. R. *J. Solid State Chem.* **1982**, *44*, 192.